# Confinement Resonances in Photoionization of Xe@$C_{60}^{+}$

A. L. D. Kilcoyne,[1] A. Aguilar,[1] A. Müller,[2] S. Schippers,[2] C. Cisneros,[3] G. Alna'Washi,[4] N. B. Aryal,[5] K. K. Baral,[5] D. A. Esteves,[5] C. M. Thomas,[5] and R. A. Phaneuf[5]

[1]*Advanced Light Source, LBNL, MS 7-100, Berkeley, California 94720-8225, USA*
[2]*IAMP, Justus-Liebig-Universität, Leihgesterner Weg 217, 35392 Giessen, Germany*
[3]*Instituto de Ciencias Físicas, UNAM, A.P. 48-3, Cuernavaca, 62251, México*
[4]*The Hashemite University, P.O. Box 150459, Zarqa 13115, Jordan*
[5]*Department of Physics, University of Nevada, Reno, Nevada 89557-0220, USA*

(Received 2 September 2010; published 15 November 2010; publisher error corrected 19 November 2010)

Experimental evidence is presented for confinement resonances associated with photoabsorption by a Xe atom in a $C_{60}$ cage. The giant 4*d* resonance in photoionization of Xe is predicted to be redistributed into four components due to multipath interference of photoelectron waves reflected by the cage. The measurements were made in the photon energy range 60–150 eV by merging a beam of synchrotron radiation with a mass/charge selected Xe@$C_{60}^{+}$ ion beam. The phenomenon was observed in the Xe@$C_{58}^{3+}$ product ion channel.

DOI: 10.1103/PhysRevLett.105.213001 PACS numbers: 32.80.Fb, 32.70.Cs, 32.80.Aa

An atom confined in a charged spherical shell is an intriguing quantum-mechanical system. The identification of endohedral fullerene molecules [1] shortly after the discovery of $C_{60}$ by Kroto and collaborators [2] has stimulated the imagination of theorists as a model system for a caged atom and the prediction of new phenomena. When a caged atom is photoionized, the emitted electron wave may be reflected by the cage, giving rise to multipath interference [3] and confinement resonances [4]. This led to a prediction by Amusia *et al.* [5,6] based on the random phase approximation with exchange (RPAE) method that the well-known broad, giant 4*d* photoionization resonance in the Xe atom [7–9] would be significantly modulated in endohedral Xe@$C_{60}$. Strong oscillations in the energy dependence of the photoionization cross section are predicted, producing four maxima while preserving an oscillator strength of 10 corresponding to the filled Xe 4*d* subshell. The $C_{60}$ cage was approximated by a $\delta$ potential with zero thickness and a radius of 0.369 nm. Because a noble-gas atom is unlikely to form ionic bonds within a $C_{60}$ molecule [10], the Xe atom was constrained to be centered within the cage.

The predictions for Xe@$C_{60}$ were subsequently reproduced by Dolmatov and Manson [11], who applied the RPAE methodology but argued that the amplitude of the oscillations depends on the thickness of the fullerene shell. They adopted a semiempirical value of 0.105 nm for the thickness of the $C_{60}$ cage [12], resulting in damping of the predicted oscillations [11].

While informative, model descriptions of $C_{60}$ by a spherical potential of zero or fixed thickness cannot fully describe the electron dynamics of such a complex multielectron system [13]. Calculations for photoionization of Xe@$C_{60}$ based on the time-dependent local-density approximation (TDLDA) were recently reported by Madjet and collaborators [14]. The TDLDA method treats the Xe atomic electrons and those of the $C_{60}$ cage within a consistent framework. Their calculation indicates some hybridization of the Xe 5*s* and 5*p* subshells and coupling to plasmon oscillations of the delocalized valence electrons of the fullerene cage [15]. Oscillatory structure due to confinement resonances is prominent in the TDLDA prediction for photoionization of the Xe 4*d* subshell.

Recent measurements by Müller and collaborators [16] of single and double photoionization of the endohedral fullerene molecular ion Ce@$C_{82}^{+}$ revealed distinct signatures of photoexcitation of the Ce 4*d* inner subshell near 125 eV, but no evidence of oscillatory structure in the cross sections due to confinement resonances. Their absence is likely explained by the fact that the Ce atom is triply ionized inside the $C_{82}$ cage. This results in hybridization of the Ce atomic orbitals and a broadening of spectral features. Density-functional theory indicates that the Ce atom is located significantly off center in the $C_{82}$ cage [17], which would further mask any signatures of multipath interference [3].

A nonreactive atom such as Xe is predicted to be centered within a $C_{60}$ cage [18]. A measurement of photoionization of Xe@$C_{60}$ in the energy range of Xe 4*d* ionization is therefore optimal for revealing evidence of confinement resonances, and for exploration of other multielectron phenomena associated with an atom in a cage. Such an experiment has not heretofore been performed because yields of synthesized noble-gas endohedral fullerenes have been low [19], precluding their purification and isolation in quantities sufficient for experiments with free endohedral molecules. Working with a mass/charge prepared fullerene ion beam greatly simplifies the isolation of trace quantities of endohedral from empty fullerenes.

Critical to the present experiment was prior preparation of samples containing Xe@$C_{60}$ based on a method reported

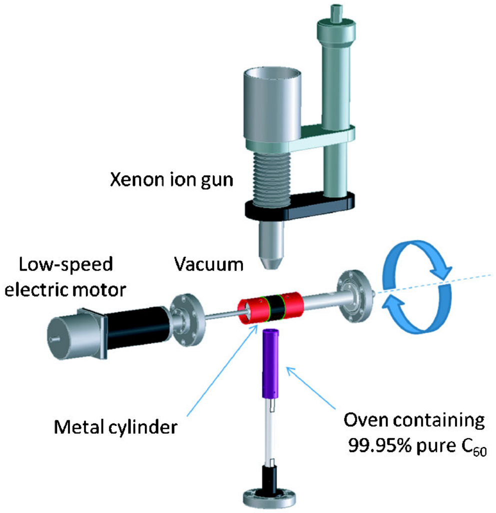

FIG. 1 (color online). Setup used to synthesize Xe@$C_{60}$ based on a method reported by Shimshi *et al.* [19].

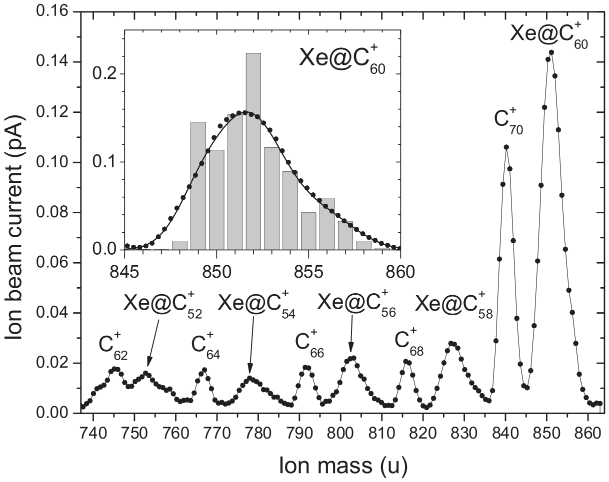

FIG. 2. Mass spectrometer scan of the ion beam from the ECR ion source operating at an Ar pressure of $5 \times 10^{-6}$ mbar, microwave power of 1 W and fullerene oven power of 12 W. The $C^+_{60}$ ion beam current (not shown) was approximately 700 pA. The inset compares the same Xe@$C^+_{60}$ peak measured with smaller steps (points) to a simulated spectrum (curve) considering the mass resolution (0.36%) and possible combinations of C and Xe isotopes weighted by their natural abundances (histogram).

by Shimshi *et al.* [19]. During a period of several months, a 150–200 eV beam of $Xe^+$ from an ion sputter gun was directed onto the surface of a rotating metal cylinder onto which 99.95% pure $C_{60}$ was continually being deposited in vacuum by evaporation from a small oven. The setup is shown in Fig. 1. The accumulated powder (few tens of mg) was scraped from the surface and placed into a small oven for evaporation into a low-power discharge in an electron cyclotron resonance (ECR) ion source. Although only a very small fraction of the $C_{60}$ molecules in the accumulated samples contained a Xe atom, this was sufficient to produce a mass/charge analyzed Xe@$C^+_{60}$ ion beam.

Figure 2 presents an ion beam mass spectrum recorded using such a prepared sample. The mass peaks corresponding to successive losses of $C_2$ dimers from $C^+_{70}$ and Xe@$C^+_{60}$ result mostly from fragmentation within the ion source discharge. Samples with estimated Xe@$C_{60}$ yields as high as $2 \times 10^{-4}$ were synthesized. The identification of Xe@$C^+_{60}$ was verified by simulating a mass spectrum considering the probable combinations of $^{12}C$ and $^{13}C$ in $C_{60}$ and the 8 stable isotopes of Xe. The natural abundances of Xe and C isotopes result in 11 possible mass numbers for Xe@$C^+_{60}$ ranging from 848 *u* to 858 *u* whose fractional abundances exceed 1%. The inset in Fig. 2 compares the measured mass peak to a simulation using natural abundances and a Gaussian to represent the mass spectrometer resolution.

Xe is theoretically predicted to form both endohedral (internal) and exohedral (external) van der Waals bonds with $C_{60}$ [20]. Evaporating 99.95% pure $C_{60}$ into the ECR ion source discharge results in $C^+_{58}$ and $C^+_{56}$ ion beam currents that are typically 15% of that of $C^+_{60}$. The situation is similar for $C^+_{70}$, giving rise to $C^+_{68}$, $C^+_{66}$, etc., as shown in Fig. 2. Survival of exohedral Xe@$C_{60}$ in such a plasma environment in which multiple pairs of C atoms are so readily removed from the $C^+_{60}$ cage seems unlikely. The Xe@$C^+_{60}$ ion beam was therefore considered to consist predominantly of endohedral molecular ions, although this could not be directly verified.

Measurements of photoionization of the Xe@$C^+_{60}$ molecular ion were performed over the photon energy range 60–150 eV using the ion-photon merged-beams end station [21] on undulator beam line 10.0.1 at the Advanced Light Source. A mass-analyzed 6 keV beam of Xe@$C^+_{60}$ ions was merged onto the axis of a counterpropagating beam of monochromatized synchrotron radiation. The beams interacted over a common path of 140 cm, after which a dipole magnet demerged the primary and product ions from the photon beam and separated them according to their charge/mass ratio. The product ions were counted by a single-particle detector as the energy of the photon beam was stepped over the range 60–150 eV at 2 eV intervals with a spectral resolution of approximately 0.2 eV.

Previous measurements of photoionization of Ce@$C^+_{82}$ in this photon energy range indicated that the product ion channels in which ionization is accompanied by the dissociation of one or more $C_2$ dimers have cross sections comparable to or larger than those for pure ionization [22]. Thus the 4*d* oscillator strength of the caged Ce ion is distributed over many product channels for single and double ionization accompanied by the loss of differing numbers of $C_2$ from the cage. The giant resonance in the neutral Xe atom near 100 eV is attributed to $4d \rightarrow \varepsilon f$ transitions [8]. Subsequent autoionization of the 4*d* hole state results in a net double ionization of Xe. Based on these considerations, the double ionization plus fragmentation product channel

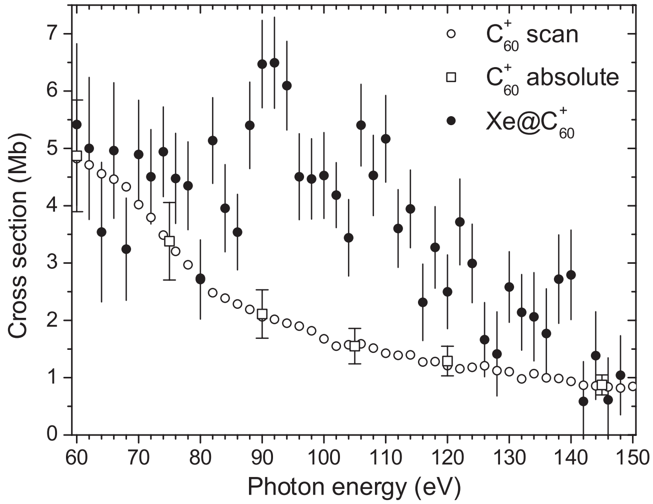

FIG. 3. Cross-section measurements for double photoionization with $C_2$ fragmentation for $C_{60}^+$ (open circles and squares) and Xe@$C_{60}^+$ (solid circles). The error bars on the solid circles are statistical (1 standard deviation from the mean), and those on the open squares are the absolute uncertainty.

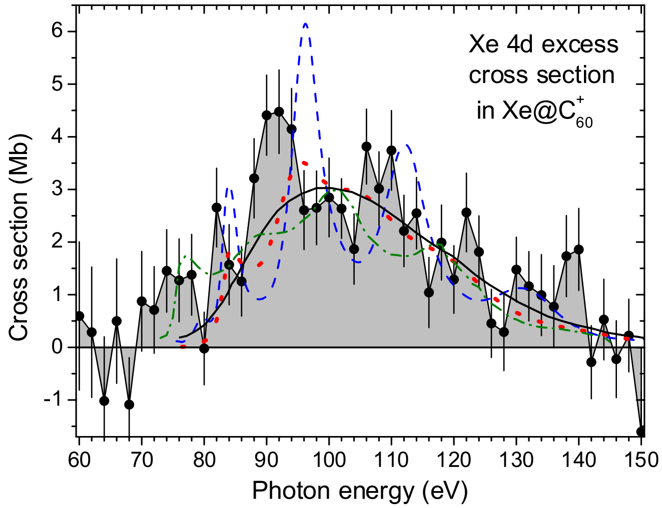

FIG. 4 (color online). Excess cross section for double photoionization accompanied by release of $C_2$ for Xe@$C_{60}^+$ relative to the same process for empty $C_{60}^+$. Error bars are statistical, representing 1 standard deviation from the mean. Plotted for comparison are RPAE theoretical cross sections for 4*d* photoionization of free Xe [8] (solid curve in black), and of Xe in a $C_{60}$ cage of zero thickness (dashed curve in blue) [5] and a cage of finite thickness (dotted curve in red) [11]. The TDLDA calculation for Xe@$C_{60}$ is shown by the dash-dotted curve in green [14]. The theoretical curves have each been divided by 10 to match the measurement—see text.

$$\gamma + \mathrm{Xe@C}_{60}^{+} \rightarrow 2e + \mathrm{Xe@C}_{58}^{3+} + \mathrm{C}_2$$

was selected for measurements in the energy range of the Xe 4*d* giant dipole resonance because it was considered likely to produce the strongest signal associated with the presence of Xe in the cage.

Figure 3 shows the present measurements for this reaction channel taken with a Xe@$C_{60}^+$ primary ion beam current ranging from 0.06 to 0.3 pA and a Xe@$C_{58}^{3+}$ product count rate in the range 0.03–0.2 Hz. The photon beam energy was stepped 33 times over the range 60–150 eV. The product ions were counted for 20 s at each photon energy during a sweep. The uncertainty in the photon energy scale is estimated to be less than 0.2 eV. Since the photon beam was mechanically chopped to subtract background counts due to collisions of the ion beam with residual gas, each solid data point corresponds to approximately 1500 s of total data accumulation at that energy. A photon energy scan under the same conditions but with the ion beam flagged verified the absence of background counts in the product ion detector produced by the photon beam. A reference absolute measurement of the cross section for double photoionization with fragmentation of the empty fullerene $C_{60}^+$ yielding a $C_{58}^{3+}$ product is also indicated and was used to normalize the Xe@$C_{60}^+$ data in the energy ranges 60–70 eV and 140–150 eV where no significant contributions from Xe 4*d* ionization are expected. Significant enhancement of the cross section for the endohedral relative to the empty fullerene between 70–140 eV is evident, as is oscillatory structure suggestive of the predicted confinement resonances.

Figure 4 presents the difference between the two measurements in Fig. 3, which is attributed to the excess cross section due to the presence of Xe inside the $C_{60}$ cage. Plotted for comparison are the RPAE calculations of cross sections for 4*d* photoionization of a free Xe atom [8], and for photoionization of Xe@$C_{60}$ predicted by Amusia *et al.* for a spherical shell of radius 0.362 nm and zero thickness [5] and by Dolmatov and Manson for a shell of radius 0.307 nm and thickness of 0.105 nm [11]. Also shown is the TDLDA calculation of Madjet *et al.* [14]. The four theoretical curves have each been divided by a factor of 10 to match the measurement. Evidently the Xe@$C_{58}^{3+}$ product channel accounts for about 10% of the Xe 4*d* oscillator strength. The experimental data indicate a strong, statistically significant enhancement of the photoionization cross section in this energy range due to the presence of Xe inside the $C_{60}^+$ cage, as well as a suggestion of oscillatory structure of amplitude and period comparable to the predictions, although shifted in energy by several eV. Static polarization of the fullerene shell due to photoionization of a caged atom has recently been predicted to produce energy shifts in the atomic photoionization spectrum [23]. It should be noted that in the calculations the cage is initially uncharged, whereas it was singly ionized in the measurement. The energy shift of the oscillatory structure in the TDLDA relative to the model-potential calculations likely results from differences in their characterizations of the fullerene shell.

The present measurements with ion beam currents of fractions of a picoampere have pushed the sensitivity of the merged-beams technique using synchrotron undulator radiation to its practical limits. On average, only a few tens of Xe@$C_{60}^+$ ions were present in the interaction region, corresponding to a target ion density of order 1 $cm^{-3}$. A statistically more definitive test of the predicted confinement resonances by this method hinges on production of noble-gas endohedral fullerenes at higher yield, and further development of methods for their synthesis is in progress.

In summary, a significant enhancement of the cross section for double photoionization accompanied by the loss of two C atoms for endohedral Xe@$C_{60}^+$ relative to that for empty $C_{60}^+$ was measured in the energy range of Xe 4*d* ionization. The data additionally show oscillatory structure due to multipath interference of Xe 4*d* photoelectron waves originating inside and transmitted or reflected by the fullerene cage.

This research was funded by the Office of Basic Energy Sciences, U.S. Department of Energy under Contract No. DE-AC03-76SF0098 and Grant No. DE-FG02-03ER15424, by the Deutsche Forschungsgemeinschaft under project Mu 1068/10, and by CONACYT-82521, Mexico.

[1] J. R. Heath *et al.*, J. Am. Chem. Soc. **107**, 7779 (1985).
[2] H. W. Kroto *et al.*, Nature (London) **318**, 162 (1985).
[3] J. Luberek and G. Wendin, Chem. Phys. Lett. **248**, 147 (1996).
[4] J. P. Connerade, V. K. Dolmatov, and S. T. Manson, J. Phys. B **33**, 2279 (2000).
[5] M. Ya. Amusia *et al.*, J. Phys. B **38**, L169 (2005).
[6] M. Ya. Amusia, A. S. Balentkov, and L. V. Chernysheva, JETP Lett. **89**, 275 (2009).
[7] Z. Altun, M. Kutzner, and H. P. Kelly, Phys. Rev. A **37**, 4671 (1988).
[8] M. Ya Amusia *et al.*, J. Phys. B **23**, 393 (1990).
[9] J. B. West *et al.*, J. Phys. B **9**, 407 (1976).
[10] M. Saunders *et al.*, Science **259**, 1428 (1993).
[11] V. K. Dolmatov and S. T. Manson, J. Phys. B **41**, 165001 (2008).
[12] Y. B. Xu, M. Q. Tan, and U. Becker, Phys. Rev. Lett. **76**, 3538 (1996).
[13] V. K. Dolmatov, in *Advances in Quantum Chemistry. Theory of Quantum Confined Systems*, edited by J. R. Sabin and E. Brandas (Academic Press, New York, 2009).
[14] M. E. Madjet *et al.*, Phys. Rev. A **81**, 013202 (2010).
[15] S. W. J. Scully *et al.*, Phys. Rev. Lett. **94**, 065503 (2005).
[16] A. Müller *et al.*, Phys. Rev. Lett. **101**, 133001 (2008).
[17] K. Muthukumar and J. A. Larsson, J. Phys. Chem. A **112**, 1071 (2008).
[18] V. V. Albert *et al.*, Int. J. Quantum Chem. **107**, 3061 (2007).
[19] R. Shimshi, R. J. Cross, and M. Saunders, J. Am. Chem. Soc. **119**, 1163 (1997).
[20] M.-S. Shon and Y. K. Sung, Chem. Phys. Lett. **245**, 113 (1995).
[21] A. M. Covington *et al.*, Phys. Rev. A **66**, 062710 (2002).
[22] A. Müller *et al.*, Bull. Am. Phys. Soc. **55**, 157 (2010).
[23] V. K. Dolmatov and S. T. Manson, Phys. Rev. A **82**, 023422 (2010).